Supplementary information for

Ross Gyre variability modulates oceanic heat supply toward the West Antarctic continental shelf

Channing J. Prend[1,2*], Graeme A. MacGilchrist[3,4], Georgy E. Manucharyan[1], Rachel Q. Pang[3], Ruth Moorman[2], Andrew F. Thompson[2], Stephen M. Griffies[3,5], Matthew R. Mazloff[6], Lynne D. Talley[6], Sarah T. Gille[6]

[1] *School of Oceanography, University of Washington, Seattle, WA, USA*

[2] *Environmental Science and Engineering, California Institute of Technology, Pasadena, CA, USA*

[3] *Atmospheric and Oceanic Sciences Program, Princeton University, Princeton, NJ, USA*

[4] *School of Earth and Environmental Sciences, University of St Andrews, St Andrews, UK*

[5] *NOAA Geophysical Fluid Dynamics Laboratory, Princeton, NJ, USA*

[6] *Scripps Institution of Oceanography, University of California San Diego, La Jolla, CA, USA*

[*] **Corresponding author**: Channing J. Prend (cprend@uw.edu)

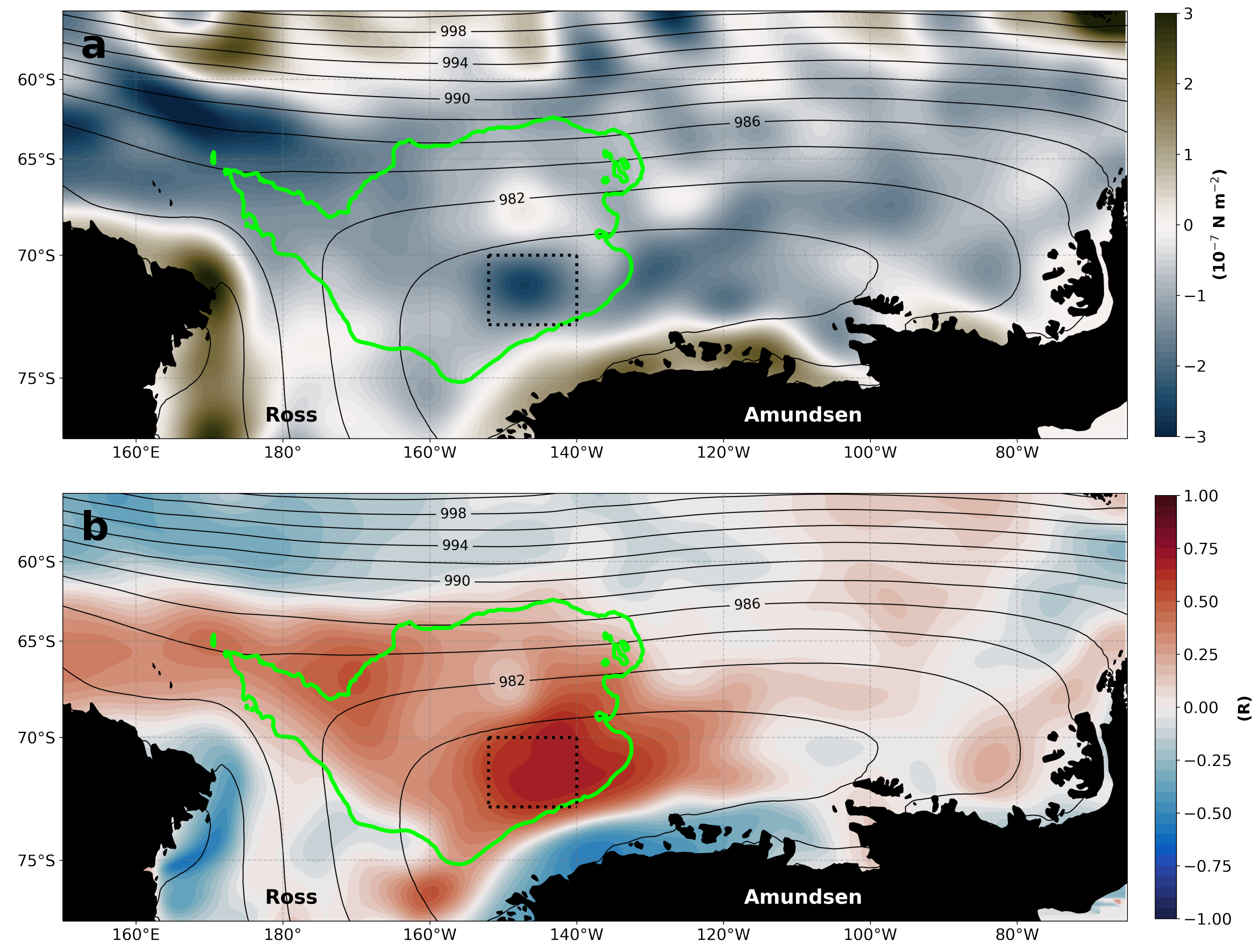

Supplementary Figure 1. (a) 2013-2018 mean ocean surface stress curl, smoothed by a Gaussian spatial filter with 2° radius. (b) Correlation coefficient between the gyre strength, defined as the mean value of the barotropic streamfunction within the −8 Sverdrup contour, and ocean surface stress curl in each grid cell. In both panels the green contour marks the mean gyre boundary and black contours denote sea level pressure. The dashed black box marks the region with high correlations (i.e. the region that most strongly forces the gyre). The ocean surface stress curl averaged over this box is presented in Fig. 2a and 6b.

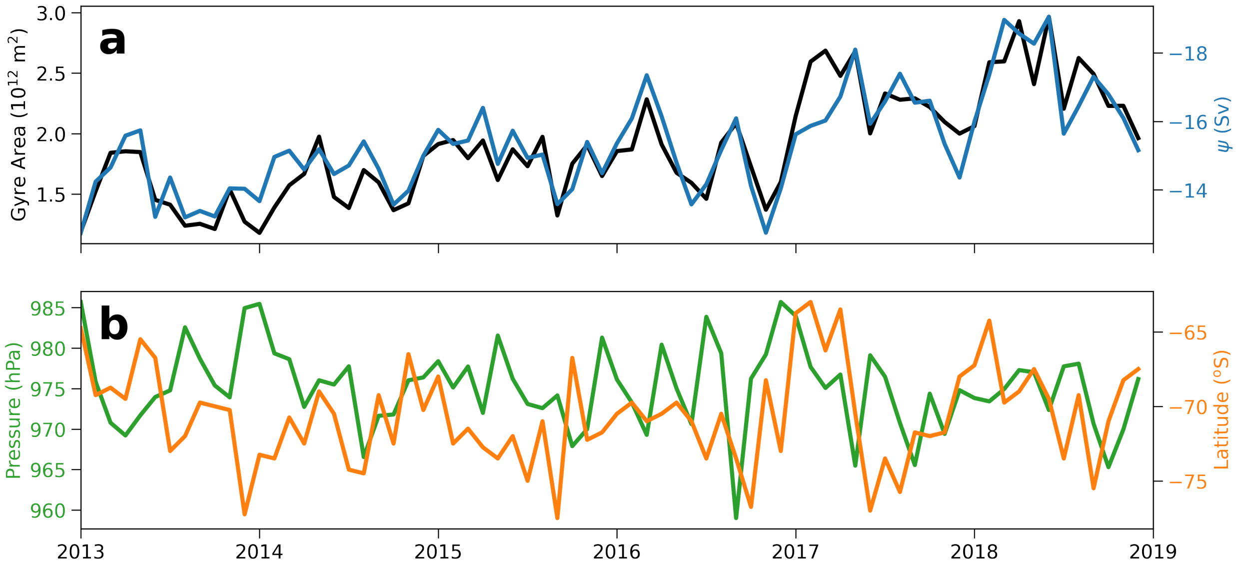

Supplementary Figure 2. (a) Monthly time series of gyre strength (blue) and area (black), defined as the mean value of the barotropic streamfunction and area enclosed by the -8 Sverdrup contour, respectively. (b) Monthly time series of Amundsen Sea Low central pressure (green), and latitude (yellow) from reanalysis data[1].

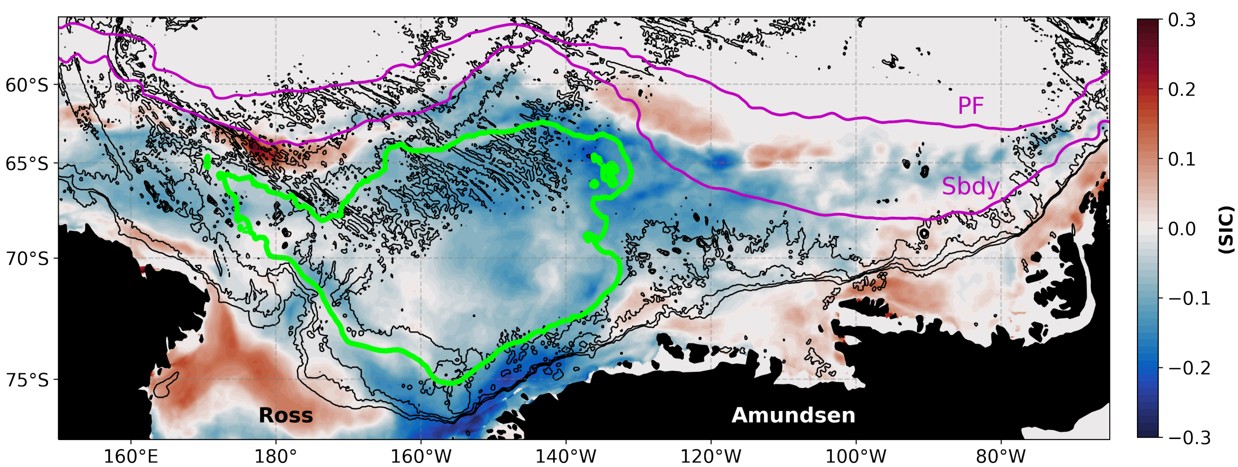

Supplementary Figure 3. 2018 minus 2014 sea ice concentration (i.e. negative values mean less sea ice in 2018 compared to 2014). Black contours mark bathymetry in 1000 m intervals and magenta lines denote the Polar Front (PF) and Southern Boundary of the Antarctic Circumpolar Current (SBdy)[2].

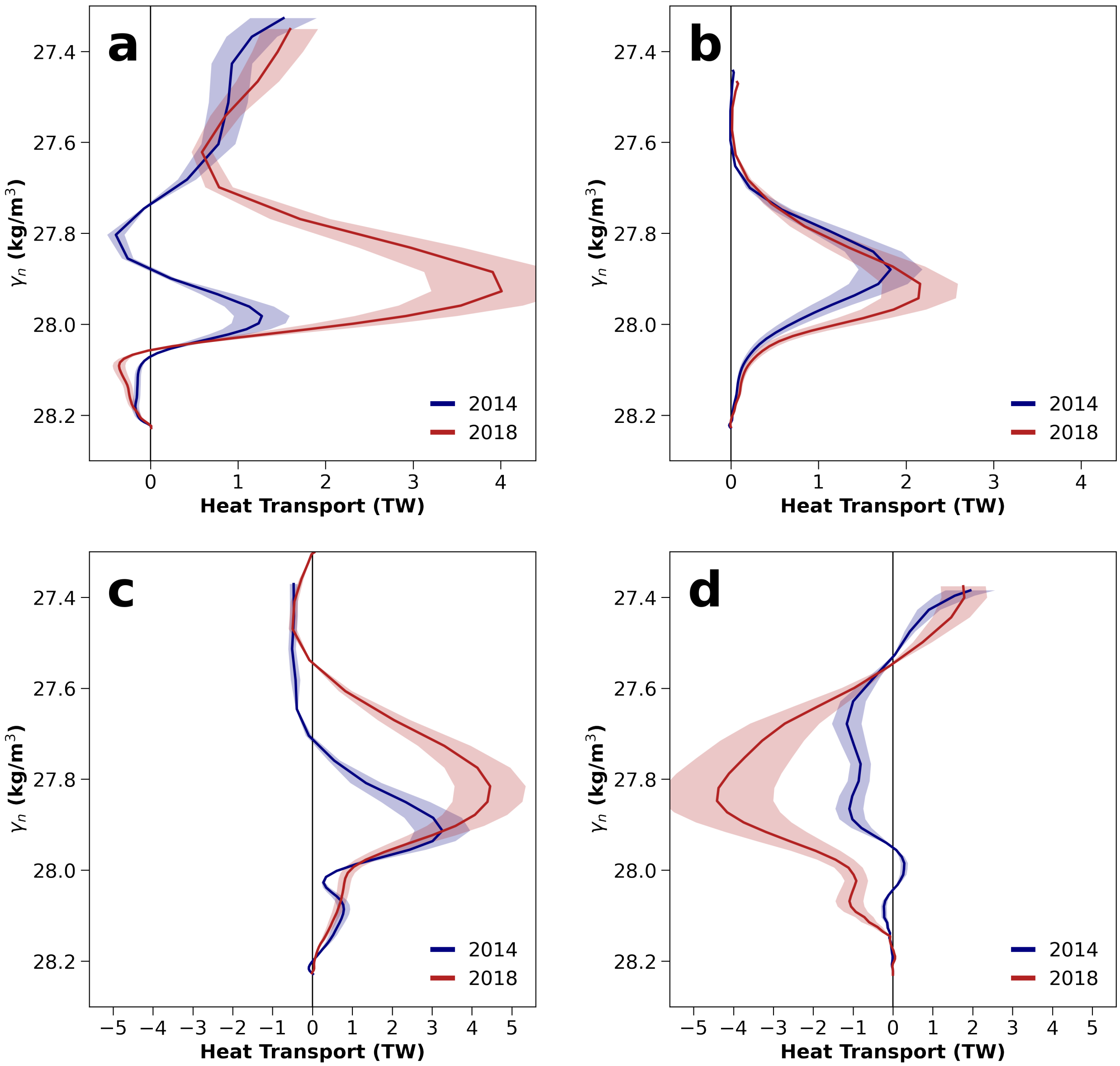

Supplementary Figure 4. Advective heat transports, defined relative to 0°C, through the (a) west, (b) east, (c) north, and (d) south faces of the offshore heat reservoir (i.e. yellow box in Fig. 6a) for 2014 (blue) and 2018 (red). A positive heat transport is defined as into the box regardless of direction. Error bars denote the standard error.

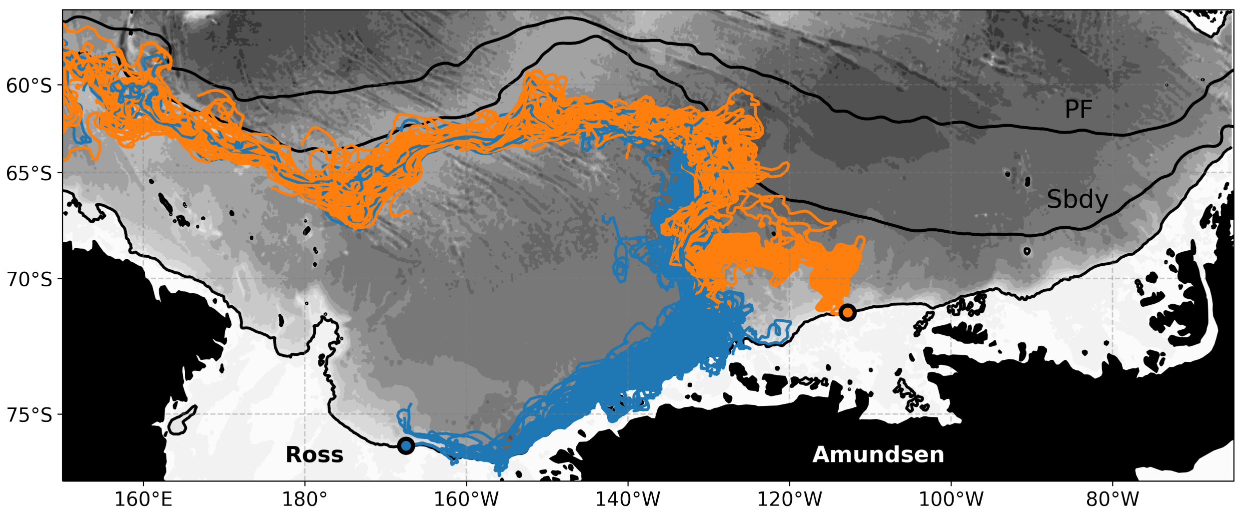

Supplementary Figure 5. (a) 100 randomly selected trajectories for particles released at the continental slope in the Ross (blue) and Amundsen (orange) and run backwards with the full model velocity fields for a 6-year integration time (for comparison with the looped velocity cases in Fig. 4). Underlying shading denotes bathymetry and black lines mark the 1000 m isobath, Polar Front (PF) and Southern Boundary of the Antarctic Circumpolar Current (SBdy)[2].

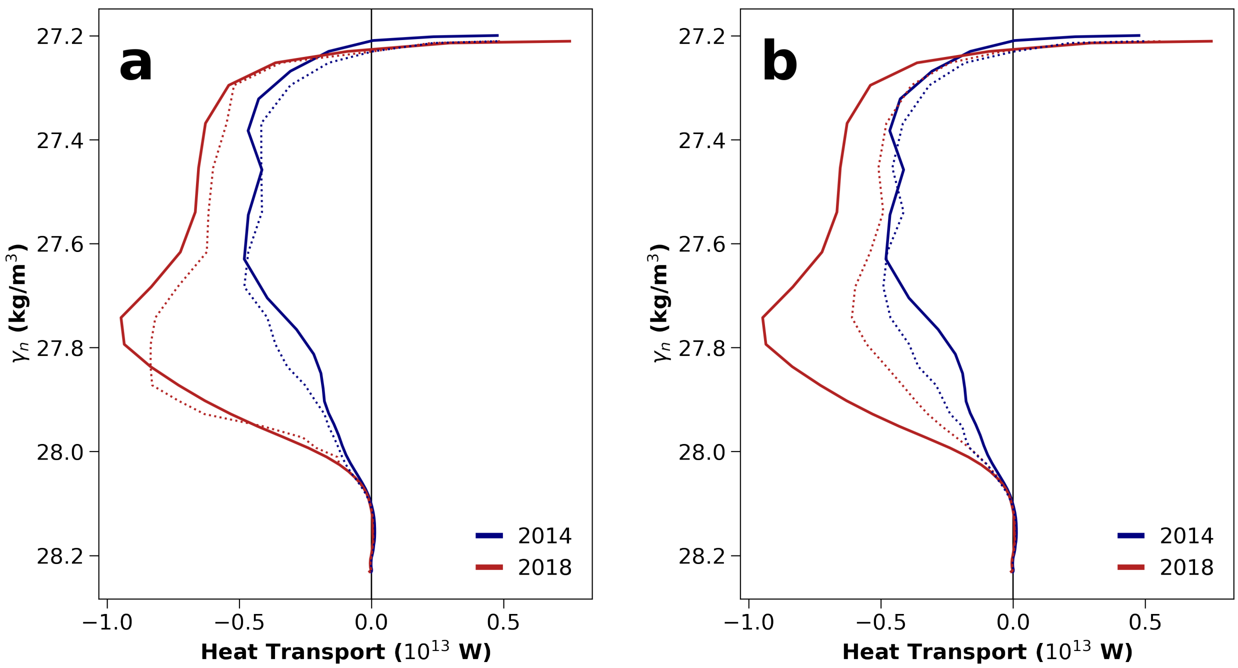

Supplementary Figure 6. Meridional heat transport, defined relative to 0°C, through the release transect (130 to 135°W at 67°S) for the two end-member years (solid) and calculated transports assuming that only velocities vary between the two years (dotted). (b) Same as (a) except dotted lines now show the calculated transports assuming that only temperatures vary between the two years. In both panels, a negative transport is southward.

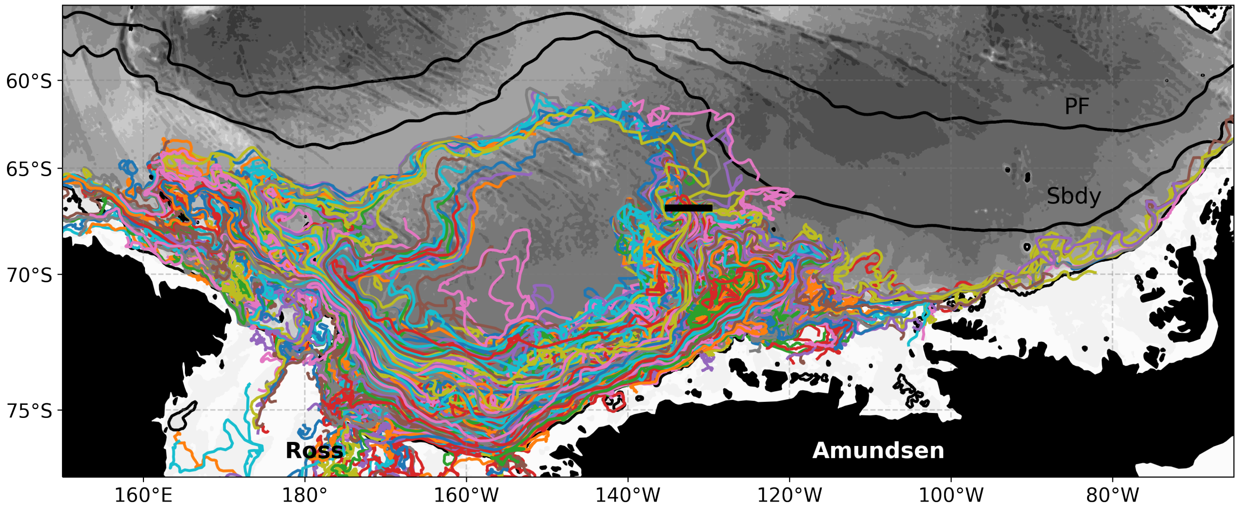

Supplementary Figure 7. 500 randomly selected trajectories for particles released at 600 m along a transect that extends from 130 to 135°W at 67°S and advected by the full model velocity fields for a 6-year integration time (for comparison with the looped velocity cases in Fig. 5). Underlying shading denotes bathymetry and black lines mark the 1000 m isobath, Polar Front (PF) and Southern Boundary of the Antarctic Circumpolar Current (SBdy)[2].

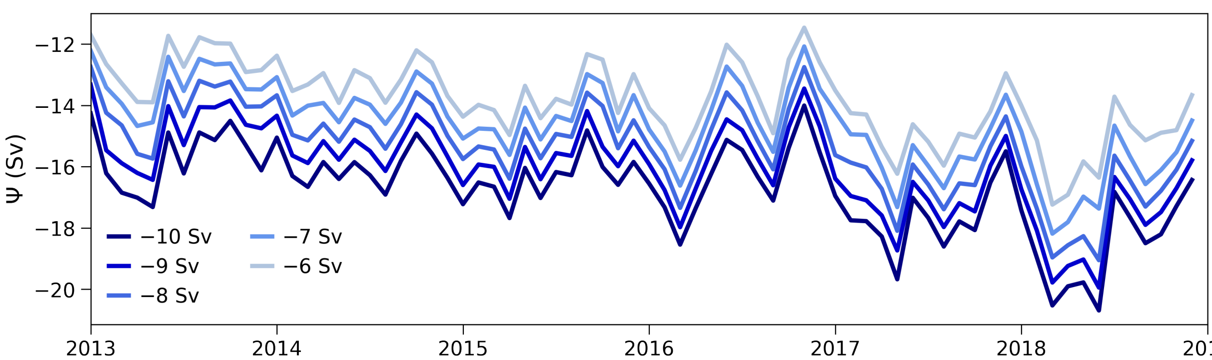

Supplementary Figure 8. Time series of gyre strength based on defining the gyre boundary using five different contours of the barotropic streamfunction. Gyre strength is taken to be the mean of the streamfunction within that contour, so the transport values will necessarily differ for each threshold. However, here we are primarily interested in the gyre's temporal variations, which are highly correlated for all threshold values (r>0.98).

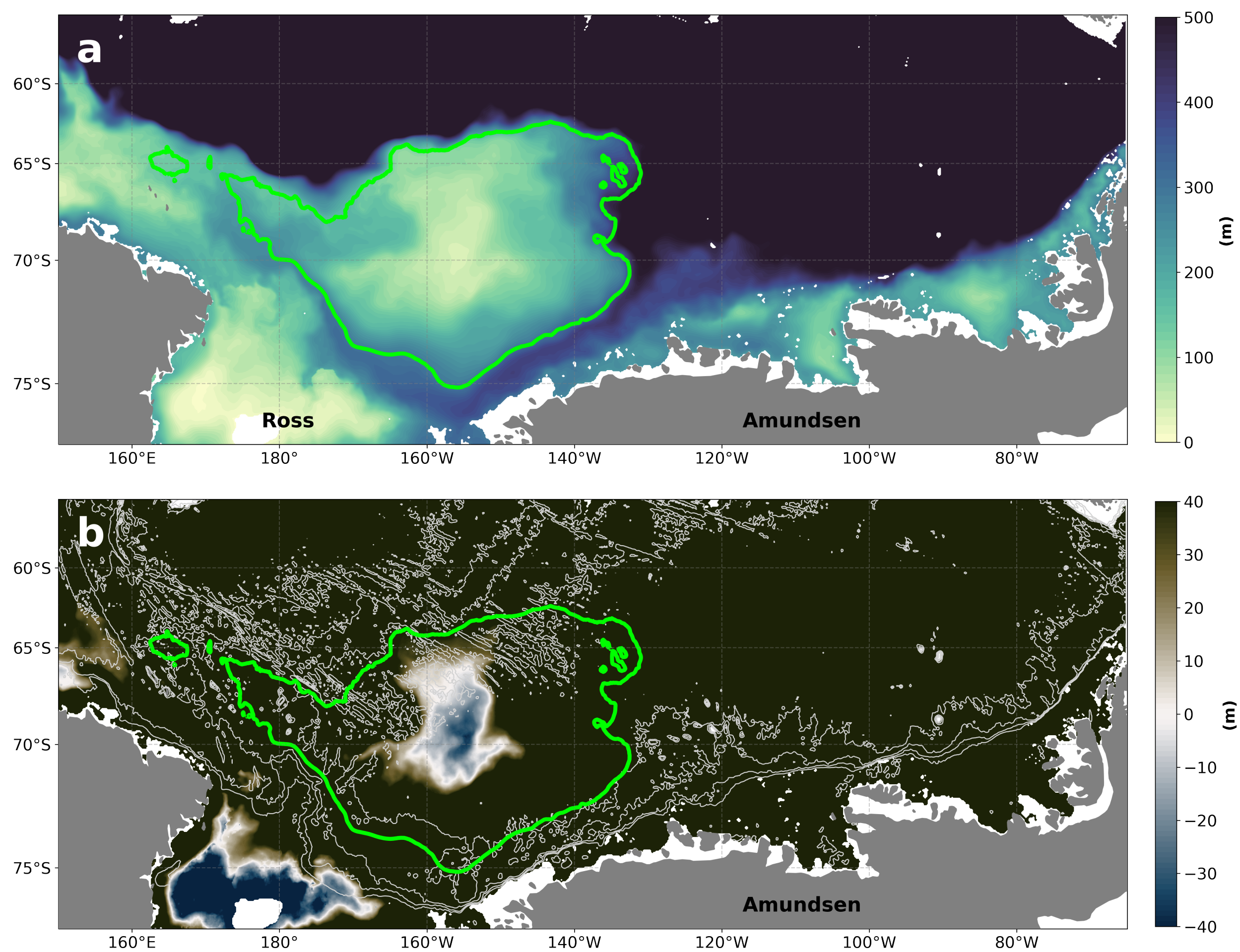

Supplementary Figure 9. (a) 2013-2018 mean depth of the $\gamma_n = 27.9$ kg m^{-3} neutral density surface in winter. (b) Difference between the isopycnal depth and the depth of the winter mixed-layer. In other words, regions that are blue (e.g. in the central gyre) are where the isopycnal outcrops into the mixed-layer in winter. In both panels, the green contour represents the mean gyre boundary. Gray lines in (b) mark bathymetry in 1000 m intervals.

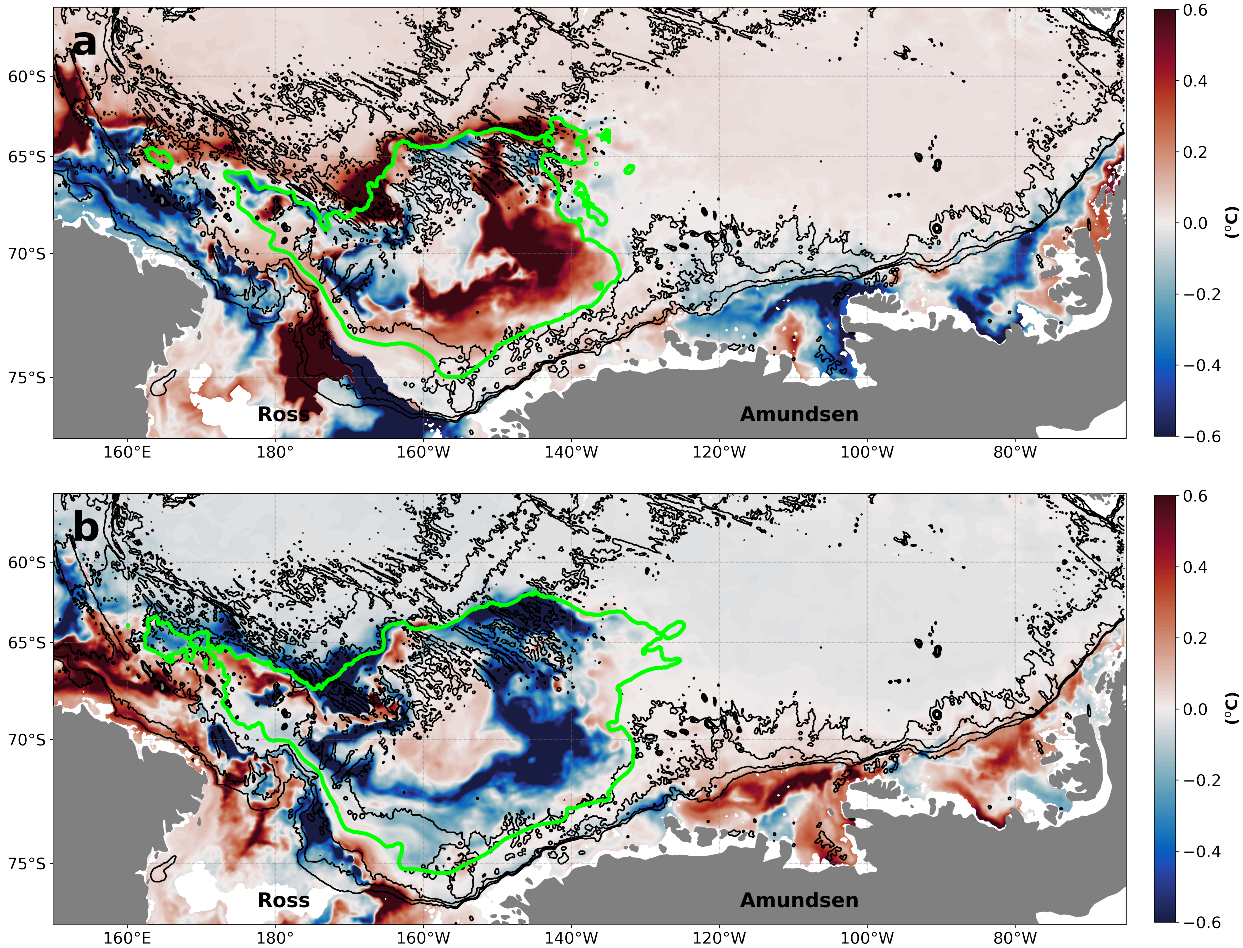

Supplementary Figure 10. Map of the annual mean temperature anomaly (relative to the 2013-2018 mean) on the $\gamma_n = 28.0$ kg m^{-3} surface for (a) 2014 and (b) 2018, reflecting the contracted and expanded gyre states, respectively. In both panels, the green contour represents the mean gyre boundary for that year, while black contours mark bathymetry in 1000 m intervals. In other words, the same as Fig. 3a,c but for a denser isopcynal.

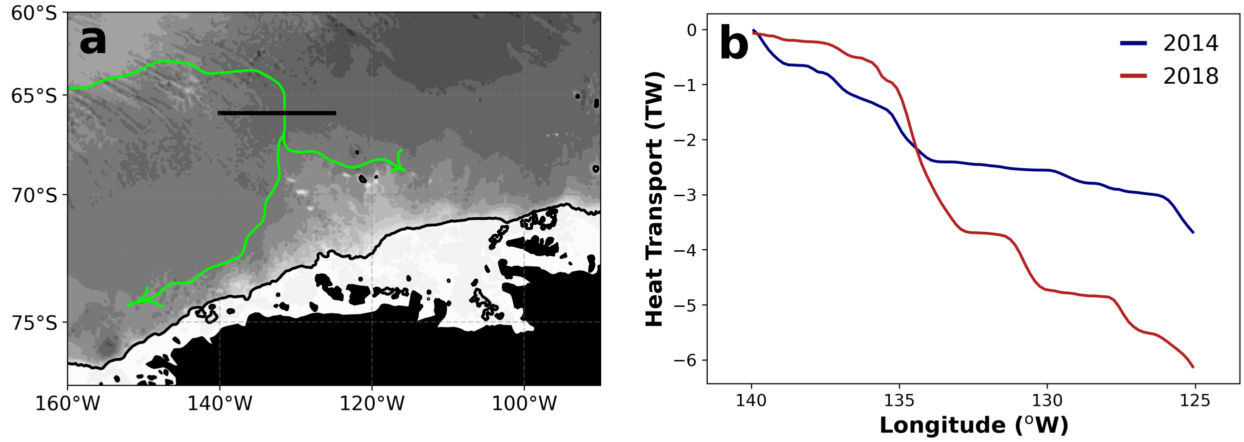

Supplementary Figure 11. (a) Map legend showing schematized version of the circulation (green arrows) and the location of the larger transect that extends from 125 to 140°W at 66°S. (b) Cumulative heat transport across this transect in the 400 to 1400 m layer plotted as a function of longitude for the two end-member years, 2014 (blue) and 2018 (red).

References

1. Hosking, J. S., Orr, A., Bracegirdle, T. J. & Turner, J. Future circulation changes off West Antarctica: Sensitivity of the Amundsen Sea Low to projected anthropogenic forcing. *Geophysical Research Letters* **43**, 367–376 (2016).

2. Kim, Y. S. & Orsi, A. H. On the variability of Antarctic Circumpolar Current fronts inferred from 1992-2011 altimetry. *Journal of Physical Oceanography* **44**, 3054–3071 (2014).